Journal of Materials Science

Effect of internal and external pressure on the phase transitions in ammonium hydrogen sulfate confined in a nanoporous glass matrix

--Manuscript Draft--

Manuscript Number:	JMSC-D-18-00622
Full Title:	Effect of internal and external pressure on the phase transitions in ammonium hydrogen sulfate confined in a nanoporous glass matrix
Article Type:	Manuscript (Regular Article)
Keywords:	Nanocomposite, Ferroelectrics, Borosilicate glass, Phase transition, Entropy, High pressure
Corresponding Author:	Igor Flerov Institut fiziki imeni Kirenskogo SO RAN Krasnoyarsk, RUSSIAN FEDERATION
Corresponding Author Secondary Information:	
Corresponding Author's Institution:	Institut fiziki imeni Kirenskogo SO RAN
Corresponding Author's Secondary Institution:	
First Author:	Igor Flerov
First Author Secondary Information:	
Order of Authors:	Igor Flerov
	Ekaterina Mikhaleva
	Andrey Kartashev
	Mikhail Gorev
	Maxim Molokeev
	Evgeniy Bogdanov
	Vitaliy Bondarev
	Leonid Korotkov
	Ewa Rysiakiewicz-Pasek
Order of Authors Secondary Information:	
Abstract:	A study of heat capacity, thermal dilatation, permittivity, dielectric loops and susceptibility to hydrostatic pressure was carried out on NH4HSO4 - porous glass nanocomposites (AHS+PG) as well as empty glass matrices. The formation of dendrite clusters of AHS with a size, dcryst, exceeding the pore size was found. An insignificant anisotropy of thermal expansion of AHS+PG showing a rather homogeneous distribution of AHS over the matrix was observed. The effect of internal and external pressures on thermal properties and permittivity was studied. At the phase transition P-1 ↔ Pc, a strongly nonlinear decrease in the entropy ΔS2 and volume strain (ΔV/V)T2 was observed with decreasing dcryst. The linear change in temperatures of both phase transitions P-1 ↔ Pc ↔ P21/c under hydrostatic pressure is accompanied by the expansion of the temperature range of existence of the ferroelectric phase Pc, while this interval narrows as dcryst decreases.
Funding Information:	Russian Foundation for Basic Research (16-32-00092 mol_a) — Dr Ekaterina Mikhaleva

Dear Editor,

We wish to submit an original research article entitled “Effect of internal and external pressure on the phase transitions in ammonium hydrogen sulfate confined in a nanoporous glass matrix” for consideration by Journal of Material Science.

We confirm that this work is original and has not been published elsewhere, nor is it currently under consideration for publication elsewhere. Publication has been approved by all co-authors.

In this paper, we report on the new original results of comprehensive study of the successive ferroelectric phase transitions in ammonium hydrosulfate embedded from the melt into nanoporous boro-silicate glasses. A significance of these investigations is associated with a problem of searching for the ways of tuning and improving the ferroelectric properties of the nanocomposite materials using the effects of internal and external pressures.

We believe that in accordance with the topics announced by Journal of Material Science this manuscript is appropriate for publication because it is devoted to development of new inorganic non-metallic nanocomposite materials on the base of glass matrix with novel functional properties of potential engineering interests.

We can suggest the following list of suitable referees:

Prof. Juras Banys
Faculty of Physics, Vilnius University, Vilnius, Lithuania
E-mail: juras.banys@ff.vu.lt
Main scientific interests are dielectric properties of ferroelectric materials, particularly in nanocomposites

Prof. Andris Sternbergs
Institute of Solid State Physics, Riga, Latvia
E-mail: stern@latnet.lv
He is a specialist in the filed of phase transitions in ferroelectric ceramics, solid solutions, etc.

Prof. Yoshihiro Hirata
Department of Chemistry, Biotechnology, and Chemical Engineering, Kagoshima University, Kagoshima, Japan
E-mail: hirata@apc.kagoshima-u.ac.jp
Main scientific interests are associated with thermal properties of solid materials with inclusions.

Thank you for your consideration of this manuscript.

Sincerely,

Igor Flerov.

Effect of internal and external pressure on the phase transitions in ammonium hydrogen sulfate confined in a nanoporous glass matrix

Ekaterina A. Mikhaleva[1], Igor N. Flerov[1,2,*], Andrey V. Kartashev[1,3], Mikhail V. Gorev[1,2], Maxim S. Molokeev[1,4], Evgeniy V. Bogdanov[1,5], Vitaliy S. Bondarev[1,2], Leonid N. Korotkov[6], Ewa Rysiakiewicz-Pasek[7]

[1]*Kirensky Institute of Physics, Federal Research Center KSC SB RAS, 660036 Krasnoyarsk, Russia,*

[2]*Siberian Federal University, 660074 Krasnoyarsk, Russia,*

[3]*Astafijev Krasnoyarsk State Pedagogical University, 660049 Krasnoyarsk, Russia,*

[4]*Department of Physics, Far Eastern State Transport University, Khabarovsk, 680021, Russia*

[5]*Krasnoyarsk State Agrarian University, 660049 Krasnoyarsk, Russia,*

[6]*Voronezh State Technical University, 394026, Voronezh, Russia*

[7]*Division of Experimental Physics, Faculty of Fundamental Problems of Technology, Wroclaw University of Science and Technology, 50-370 Wroclaw, Poland*

* Corresponding author **Igor Flerov**

flerov@iph.krasn.ru

Tel: +7 (391) 24945 07

Kirensky Institute of Physics,

Akademgorodok, 50, bld. 38

Krasnoyarsk, 660036, Russia

e-mail addresses of co-authors:

Ekaterina A. Mikhaleva:	katerina@iph.krasn.ru
Andrey V. Kartashev	akartashev@yandex.ru
Mikhail V. Gorev	gorev@iph,krasn.ru
Maxim S. Molokeev	msmolokeev@mail.ru
Evgeniy V. Bogdanov	evbogdanov@yandex.ru
Vitaliy S. Bondarev	vbondarev@yandex.ru
Leonid N. Korotkov	l_korotkov@mail.ru
Ewa Rysiakiewicz-Pasek	Ewa.Rysiakiewicz-Pasek@pwr.edu.pl

Abstract

A study of heat capacity, thermal dilatation, permittivity, dielectric loops and susceptibility to hydrostatic pressure was carried out on NH_4HSO_4 - porous glass nanocomposites (AHS+PG) as well as empty glass matrices. The formation of dendrite clusters of AHS with a size, d_{cryst}, exceeding the pore size was found. An insignificant anisotropy of thermal expansion of AHS+PG showing a rather homogeneous distribution of AHS over the matrix was observed. The effect of internal and external pressures on thermal properties and permittivity was studied. At the phase transition $P\text{-}1 \leftrightarrow Pc$, a strongly nonlinear decrease in the entropy ΔS_2 and volume strain $(\Delta V/V)_{T2}$ was observed with decreasing d_{cryst}. The linear change in temperatures of both phase transitions $P\text{-}1 \leftrightarrow Pc \leftrightarrow P2_1/c$ under hydrostatic pressure is accompanied by the expansion of the temperature range of existence of the ferroelectric phase Pc, while this interval narrows as d_{cryst} decreases.

Keywords: Nanocomposite, Ferroelectrics, Borosilicate glass, Phase transition, Entropy, High pressure

1. Introduction

Despite the wide popularity of porous glasses due to the possibility of their use in various scientific studies and many industrial applications, there is a series of questions and problems related to their preparation, certification and, especially, application [1,2]. Recently, a special attention was paid to the porous glasses as a basis for creating composite materials. A lot of publications appeared describing the researches of glass matrices with embedded materials of various nature, in particular ferroelectrics. In the latter case, the main direction of research of glass composites was, as a rule, associated with the study of behavior of the dielectric properties of the ferroelectric component in confined geometry, and its dependence on a type of the matrices and diameter of the pores [3-10]. Other properties, in particular thermodynamic, have been examined to a lesser extent. At the same time, the study of the heat capacity and thermal dilatation of composites provides information on the effect of interaction between components of composites on entropy and deformation associated with the ferroelectric phase transitions [9,11-14]. The effect of external pressure on the ferroelectric nanocomposites has not been examined at all. Recently it has been shown that high-pressure is a very powerful tool to modify nanostructured materials, study interactions at the nanoscale and design new nanomaterials [15].

In this connection the data on the heat capacity and thermal dilatation of the nanoporous matrices are also very important. However, as far as we know, thermodynamic properties of porous glasses were not studied systematically.

This paper presents the results of studies of nanocomposites prepared on the basis of ammonium hydrogen sulfate, NH_4HSO_4, embedded into borosilicate glass matrices. We intended to analyze the effect of internal pressure associated with the confined geometry as well as hydrostatic pressure on the entropy, elastic strain and baric coefficients of the phase transitions in ferroelectric component. For this purpose, the heat capacity, thermal dilatation, dielectric properties and susceptibility to external hydrostatic pressure of the nanocomposites were investigated. To be correct when analyzing data on the properties of ferroelectric component, heat capacity and thermal expansion of the nanoporous glasses were also studied. The originality of our investigations compared to recent studies [9,12,14] of heat capacity and permittivity of nanocomposites with NH_4HSO_4 is associated with the following points:

1) the porous glasses were filled with molten NH_4HSO_4 to reliably avoid the presence of an aqueous solution in the pores;
2) studies of the heat capacity were performed using an adiabatic calorimeter showing high resolution and high stability of measurements instead of the low sensitive differential scanning calorimeter [14];
3) permittivity was studied at atmospheric and high pressures;
4) investigations of thermal dilatation and the effect of pressure on phase transitions are pioneering;
5) detailed studies of the thermodynamic properties of porous borosilicate glasses were carried out.

The choice of the object of research is due to several reasons. First, NH_4HSO_4 undergoes a succession of the phase transitions P-1($P1$) (T_2 = 160 K) ↔ Pc (T_1 = 271.7 K) ↔ $P2_1/c$ of the first and second order, respectively [16-18]. (Two possible space groups for the phase at T < T2 are presented, since there is still no consensus on the nature of the corresponding structural transformation.) Second, previously we have carried out studies of the effect of chemical pressure on phase transitions, as well as electro- and barocaloric effects in solid solutions $(NH_4)_{1-x}Rb_xHSO_4$ [19]. Third, in the manufacture of composites, we used an important advantage of NH_4HSO_4, in comparison with other water-soluble ferroelectrics, associated with the possibility of its melting without decomposition. Recent comparative studies of the NH_4HSO_4 samples prepared from an aqueous solution and the melt have shown quite similar thermodynamic and dielectric properties [20].

2. Sample preparation and measurement technique

Hereinafter, NH_4HSO_4, borosilicate porous glasses and NH_4HSO_4-glass nanocomposites will be labeled as AHS, PG and AHS+PG, respectively. For the present study we have used PGs with five different pore sizes. The samples of the glass matrices with average diameter of pores 23, 46, 160, and 320 nm were cut out in the form of flat plates of about 1.0×1.0×0.05 cm^3. The volume of PG with pores 5 nm in diameter (PG5) was 0.291 cm^3. The porosity was determined by the relative mass decrement method during the preparation of the samples as well as evaluated by adsorption of a water stream and a mercury intrusion porosimetry. The pore sizes were determined in the framework of a cylindrical pore model. The methods of certification of samples studied one can also see in [1]. The porosity of different PGs was found in the range of 40 – 55% (Table 1).

The nanocomposites AHS+PG were fabricated by immersion of empty PG into the melted AHS for several hours. To avoid the non-equilibrium state in AHS observed by [21], subsequent cooling down to room temperature was carried out at a very low rate (~ 0.1 K/min). A mechanical polishing was used to remove micro-crystals from the surfaces of the composite samples. The filling factor was estimated as the ratio of the volumes of the embedded AHS to the pores volume (Table 1). For dielectric measurements silver electrodes were painted onto the samples' surfaces.

Table 1 Characteristics of porous glasses and nanocomposites. d_{pore} and d_{cryst} are the sizes of pores and nanoparticles, respectively

Glasses		Nanocomposites	
d_{pore} (nm)	Porosity (%)	Filling factor (%)	d_{cryst} (nm)
5	42	38	9.0(4)
23	55	90	70(2)
46	55	67	47(2)
160	46	81	500(39)
320	50	74	115(15)

Characterization of AHS, PG and AHS+PG was carried out at room temperature by XRD using a Bruker D8 ADVANCE powder diffractometer (Cu-Kα radiation). Fig. 1a depicts a

diffraction pattern of PG46, which is typical for the other samples of PG and for the amorphous materials without any crystalline phases. The results of Rietveld refinement for the samples AHS and AHS+PG46 are shown in Fig.1(b)-(c). No additional phases were observed in ammonium hydrogen sulfate as well as in all the nanocomposites. The information on the ferroelectric nanoparticles size, d_{cryst}, filling the pores of matrix was obtained using TOPAS 4.2 program [22]. The high reliability of the obtained data is confirmed by relatively small values of estimated standard deviation presented in Table 1 which shows that an increase in the pore diameter is not accompanied by monotonic increase in d_{cryst}. Moreover, in the case of three composites with PG5, PG23 and PG160, d_{cryst} exceeds the pore diameter. Recently, similar situation observed in nanocomposites with the embedded $NaNO_2$ was explained as associated with the formation of the dendrite clusters in pores [4].

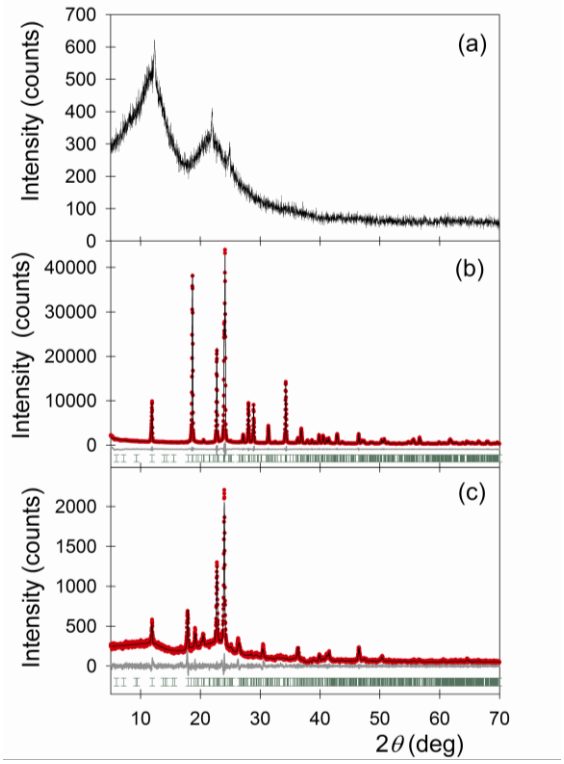

Figure 1 XRD patterns: (**a**) empty PG46; (**b**) AHS; (**c**) AHS+PG46.

The micromorphology of the surface of empty glasses and nanocomposites was examined using scanning electron microscopes (SEM) Hitachi TM3000 and Hitachi S-5500 (Hitachi High-Technologies Co., Ltd., Tokyo, Japan). The typical SEM images of the samples PG5, PG46 and AHS+PG46 are shown in Fig. 2. One can see noticeable loss of the image contrast in nanocomposites.

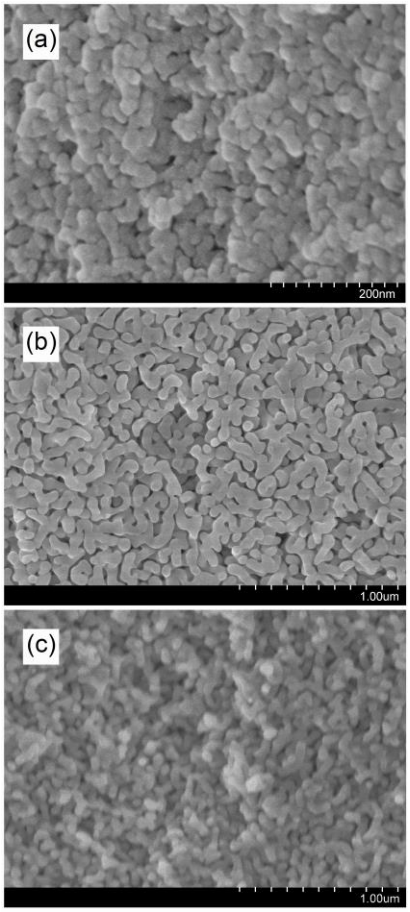

Figure 2 SEM images: (**a**) PG5; (**b**) PG46; (**c**) AHS+PG46.

In order to perform a correct analysis of the properties of AHS nano-sized crystals embedded into the glass matrix, it is necessary to have information on the properties of glass matrices and AHS. Recently, we have studied thermodynamic properties of bulk AHS prepared from an aqueous solution and the melt and found that parameters characterizing both phase transitions are close to each other for the both samples [20]. To our knowledge, the data on thermodynamic properties of boron-silicate glasses are absent. So first of all we studied the heat capacity and thermal dilatation of PGs which were then filled with AHS.

Measurements of thermal expansion were performed using a push-rod dilatometer (NETZSCH model DIL-402C) with a fused silica sample holder. Experiments were carried out in the temperature range 100 – 300 K with a heating rate of 3 K/min in a dry He flux. The results were calibrated, by taking quartz as the standard reference, to remove the influence of system thermal expansion. Because of a large difference in thermal dilatation of PG and AHS, the uncertainty in measurements was individual, about 20% for PG and 8% for AHS+PG. However, the reproducibility of data obtained in successive series of all the measurements was not less than 5%.

Measurements of the heat capacity of samples examined in dilatometric experiments were performed in a wide temperature range of 82–300 K by means of a homemade adiabatic calorimeter with three screens, as described by [23]. The inaccuracy in the heat capacity determination did not exceed 0.5–1.0%. The heat capacity of the "sample+heater+contact grease" system was measured using discrete as well as continuous heating. In the former case, the calorimetric step was varied from 1.5 to 3.0 K. In the latter case, the system was heated at rates of $dT/dt \approx 0.15–0.30$ K/min. The heat capacities of the heater and contact grease were determined in individual experiments.

Dielectric properties were also studied in an adiabatic calorimeter. The temperature behavior of the permittivity ε was investigated using an E7-20 immittance meter at frequencies from 1 Hz up to 10^6 Hz while heating at a rate of about 0.5 K/min. The dielectric hysteresis (*P-E* loop) was examined using an aixACCT EASY CHECK 300 technique. The driving-field profile was a triangular wave of amplitude E_{max} = 5 kV/cm. The frequency of the measuring electric field was 250 Hz. Measurements of ε(*T*) were performed only on nancomposites because similar investigations on AHS [20] and empty PG [9] were carried out recently. In the latter case, it was shown that permittivity of PG does not depend significantly on temperature (in the range 120 – 400 K) and frequency at least up to $f = 10^6$ Hz.

The effect of hydrostatic pressure on the phase transitions in AHS component embedded in PG was studied using a piston-cylinder type vessel associated with a pressure multiplier. Pressure of up to 0.25 GPa was generated using pentane as the pressure-transmitting medium. The inaccuracy in the measurements of pressure and temperature using a manganin gauge and a copper-constantan thermocouple was about $\pm 10^{-3}$ GPa and ±0.3 K, respectively.

The dependences $T_1(p)$ and $T_2(p)$ were studied by measuring both permittivity and the differential thermal analysis (DTA) signal. In the former case, the measurements were preformed using the technique used in the studies at atmospheric pressure and described above. In the latter case, a germanium-copper thermocouple characterized by high sensitivity to change in temperature (~ 400 μV/K) was used [24]. Two junctions of the thermocouple were formed by soldering a copper wire 0.08 mm in diameter to a germanium bar of 0.5 × 2.0 × 5.0 mm^3 dimensions. A sample of 0.5 × 4.0 × 4.0 mm^3 dimensions was glued onto one of the two junctions of a thermocouple. A quartz sample cemented to the other junction was used as a reference substance. To ensure the reliability of the results, the measurements were performed for both increasing and decreasing pressure cycles.

3. Results and discussion

Fig. 3a depicts the temperature dependences of the specific heat, $C_p(T)$, of PGs. Difference in the chemical composition of the borosilicate glasses studied is not significant and as a result one can see a rather good agreement between the data for the samples with average diameter of porous 5, 46, and 320 nm in the whole temperature range examined, 100 – 300 K. The maximum difference between curves $C_p(T)$ observed at about 100 K does not exceed several percents.

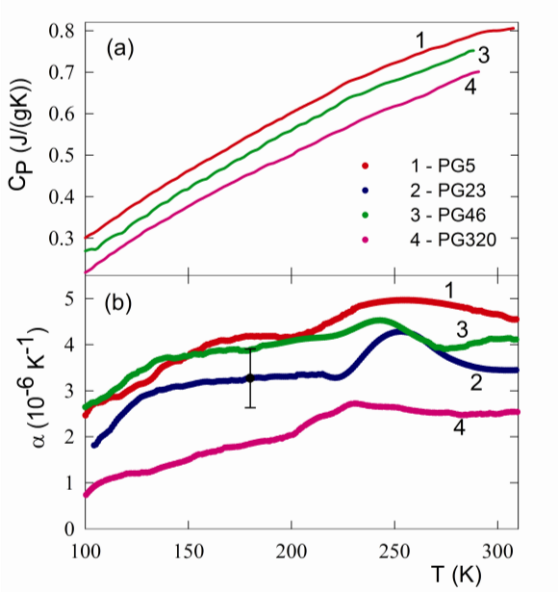

Figure 3 Temperature dependences of: (**a**) the specific heat (curves 3 and 4 are shifted down at 0.05 and 0.10 J×(g×K)$^{-1}$, respectively); (**b**) the coefficient of linear thermal expansion of PGs.

In contrast to the specific heat, thermal dilatation of PGs was found dependent on the pore size (Fig. 3b). The largest and smallest values of the coefficient of linear thermal expansion, α, are characteristic for PG5 and PG320, respectively, and differ from each other almost in two times. However, taking into account very small α value of PGs and as a result increased inaccuracy in their determination, one can think that the difference observed is not so large.

All the α(T) dependences of PGs demonstrate a bump in rather wide temperature range ~(220 - 290) K. We think that it can be associated with a small amount of water left in the pores because of ambient pressure of the α measurements. Due to a high vacuum (~10^{-6} mm Hg) in experimental chamber of the adiabatic calorimeter, no anomalies on the $C_p(T)$ dependences of PGs were observed (Fig. 3a).

Experimental data obtained by adiabatic calorimeter for AHS+PG nanocomposites are shown in Fig. 4a. The temperature dependences of the heat capacity demonstrate pronounced anomalies associated with the phase transition $P\text{-}1 \leftrightarrow Pc$ at T_2. Due to small heat capacity change at T_1 even in pure molten AHS [20] the anomalies of $C_p(T)$ in nanocomposites in the region of the $Pc \leftrightarrow P2_1/c$ transformation are decreased and smeared.

To obtain information on the phase transition entropies, the anomalous contribution, ΔC_p, to the total heat capacity C_p was extracted. This procedure was carried out using a polynomial functions describing nonanomalous heat capacity of the nanocomposites consisted of lattice heat capacity of AHS and $C_p(T)$ of PG, $C_{reg} = C_L + C_{PG}$. For this aim, the experimental data $C_p(T)$ of AHS+PG were taken far from the transition points in AHS component (T < 145 K and T > 273 K) as it was done during the analysis of the heat capacity of bulk AHS [20]. In all the cases, the average deviation of the experimental data from the smoothed curves does not exceed 1.5%. The regular contributions into the total heat capacities of the nanocomposites are shown as a dashed line in Fig. 4a. One can see that the degree of the smearing as well as decreasing both anomalies changes with the pore size change.

The total excess entropy $\Sigma\Delta S = \Delta S_1 + \Delta S_2$ associated with the successive phase transitions P-1 ↔ Pc ↔ $P2_1/c$ was determined by integrating the area below the $\Delta C_p/T$ versus T curves taking into account the mass of AHS in each of the nanocomposites. Fig. 4b shows the temperature behavior of $\Sigma\Delta S$ in AHS confined in PGs. there is a significant decrease in $\Sigma\Delta S$ values with decrease in pore size or nanoparticle size. This suggests a decrease in the disordering of structural elements in the initial phase $P2_1/c$ of AHS confined in glass matrix. In addition, a strong smearing of the change in entropy at T_1 and T_2 was also observed which can be associated with heterogeneity of the sizes of pores as well as crystallites.

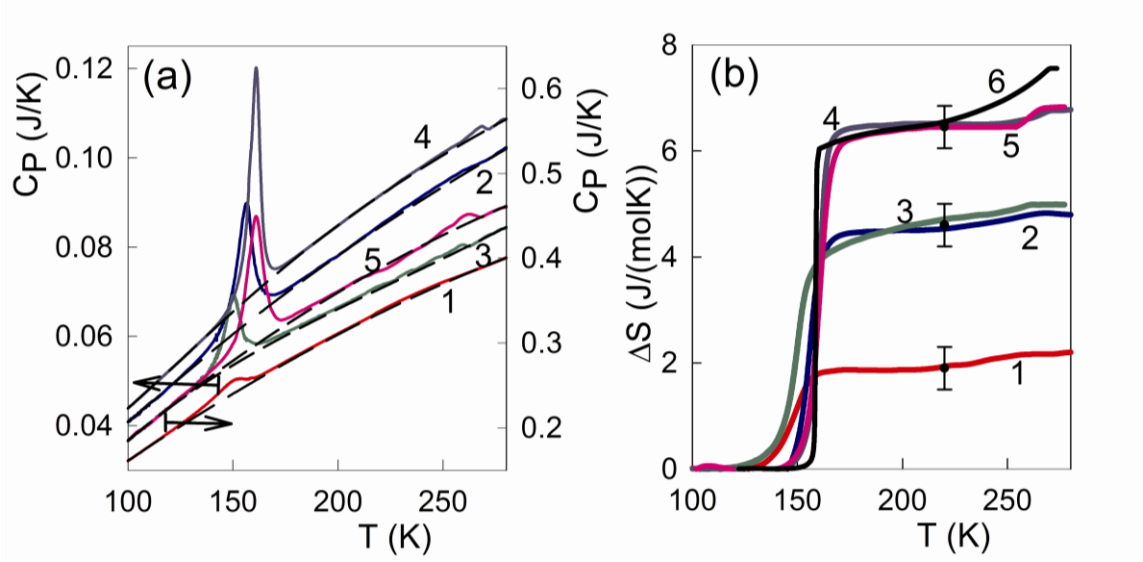

Figure 4 (**a**) Temperature dependences of the heat capacity of the nanocomposites. The dashed lines are the regular heat capacities. (**b**) Behavior of the excess entropy associated with the P-1 ↔ Pc ↔ $P2_1/c$ phase transitions in AHS component. 1- AHS+PG5, 2 - AHS+PG23, 3 - AHS+PG46, 4 - AHS+PG160, 5 - AHS+PG320, 6 – AHS.

Linear thermal expansion coefficient $\alpha \approx (27 – 70)\times10^{-6}$ K^{-1} of AHS in the temperature ranges far from the phase transition points [17,20,25] is many times as much compared to $\alpha \approx$

(1–5)×10^{-6} K^{-1} of empty PGs (Fig. 3b). A large difference in α of the matrix and AHS can lead to an increase of α of AHS+PG compared to PGs and to the appearance of intrinsic elastic stress which will change at temperature variation. However, because PGs were filled with AHS at about 430 K, further cooling down to room temperature and below should be accompanied by more rapid decrease in the volume of AHS compared to PG and, as a result, tensile stresses can appear in the elastic interactions between two components which will increase upon cooling and decrease upon heating.

The results of dilatometric measurements on nanocomposites are presented in Fig. 5. In the temperature regions of nonanomalous behavior of the thermal expansion, one can see a distinct difference between the α values for the different AHS+PG samples (Fig. 5a) which is due to the different filling factor, the nanoparticle size (Table 1) and, to a lesser extent, the difference in the α values of PGs (Fig. 3b). Indeed, the filling factor is, for example, about 38% and 90 % for AHS+PG5 and AHS+PG23, respectively, and this determines the smallest (2.5×10^{-6} K^{-1}) and largest (36×10^{-6} K^{-1}) values of α at 300 K.

Fig. 5b demonstrates the α(*T*) dependences of PG320 and AHS+PG320 revealing that a linear coefficient of the thermal expansion of the AHS+PG samples is several times greater than α of PG. These data are given by way of example, but are true for all the nanocomposites studied. Such an effect of AHS on the thermal expansion of nanocomposites can be associated only with a strong elastic interaction between the ferroelectric and the glass components.

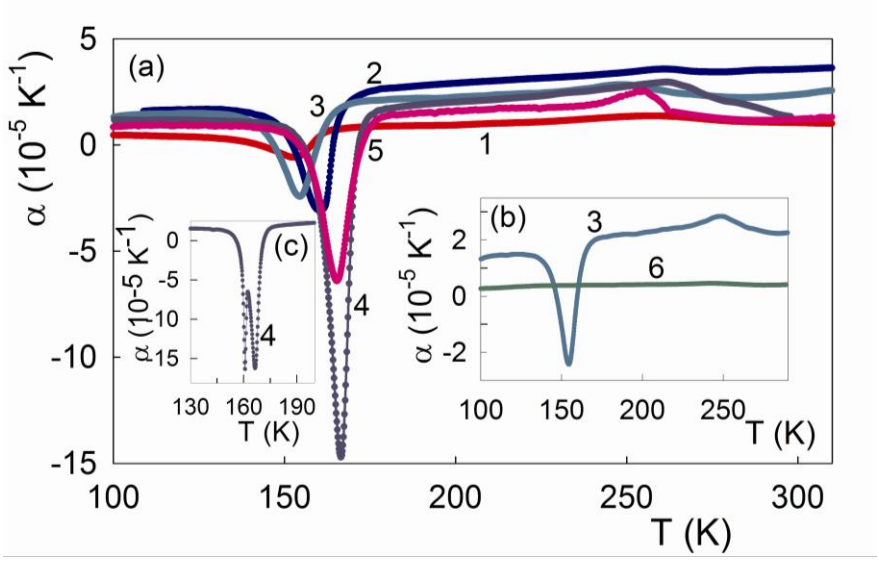

Figure 5 (**a**) Temperature dependences of the thermal expansion coefficient of the nanocomposites; 1 - AHS+PG5, 2 - AHS+PG23, 3 - AHS+PG46, 4 - AHS+PG160, 5 - AHS+PG320, 6 – PG46. (**b**) Comparison of α for AHS+PG46 and PG46. (c) Thermal dilatation around T_2 in the AHS+PG160 sample with part of the melt on its surface.

Nanocomposites under study consist of an isotropic glass matrix and a crystalline ferroelectric with monoclinic symmetry in initial room temperature phase. To check the effect of an anisotropic component on the thermal expansion of a composite based on an isotropic matrix, we performed measurements of α in three directions on AHS+PG320: along two sides of the plate and perpendicular to its largest surface. The difference in α for different directions did not exceed 10-15 %. Taking into account the inaccuracy of dilatometric measurements, the distribution of AHS over the volume of the nanocomposites can be considered as statistically uniform with equiprobable orientations of crystalline nanoparticls in all directions.

One of the features of the nanocomposites studied is that the temperatures, T_1 and T_2, of phase transitions are characterized by a nonmonotonic change with decreasing pore size. Fig. 6a depicts dependences of the both phase transition temperatures on the size of nanoparticles in comparison with the values for bulk AHS [20]. A reduction of d_{cryst} from 500 nm down to 9 nm is accompanied by narrowing of the temperature region of ferroelectric *Pc* phase existence.

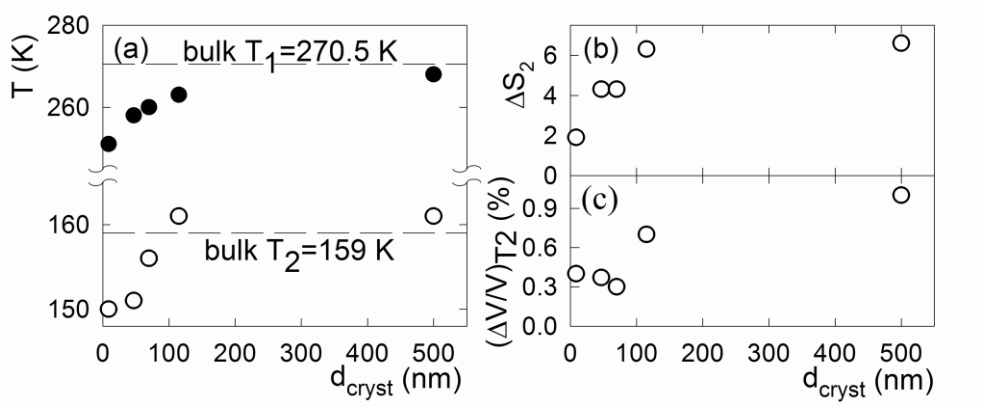

Figure 6 Effect of the nanoparticle size of AHS on (**a**) phase transitions temperatures in nanocomposites AHS+PG and the change in (**b**) entropy ΔS_2 (J/mol×K)) and (c) volume strain $(\Delta V/V)_{T2}$ at the *P*-1 ↔ *Pc* transformation

The behavior of the temperatures of phase transitions in nanocomposites demonstrates very interesting general and specific features. At $d_{cryst} \leq 100$ nm, T_1 and T_2 strongly decrease with decreasing nanoparticle size. In all nanocomposites, the temperature of the phase transition *Pc* ↔ $P2_1/c$ is lower than T_1 in the bulk AHS. At that time, T_2 in AHS+PG160 and AHS+PG320 exceeds the bulk value (Fig. 6a). To verify the latter effect, we left part of the AHS melt on the surface of the AHS+PG160 sample and performed measurements of α(*T*). Fig. 5c demonstrates two peaks on the α(*T*) curve associated with the *P*-1 ↔ *Pc* phase transition in the AHS component and the bulk AHS on the surface of the sample. Thus, there really is a difference in the values of T_2 in the "free" and confined AHS. Below we return to discussing the features above in the behavior of T_1 and T_2 in comparison with the effect of hydrostatic pressure.

Experimental data on $\alpha = L^{-1} \times (\Delta L/\Delta T)$ are presented in Fig. 5a for a number of nanocomposites, where L is the linear dimension of the glass matrix plate. To obtain information on the change in the volume strain at the first-order transition $P\text{-}1 \leftrightarrow Pc$ in the AHS component, we recalculated α into volume strain $(\Delta V/V)_{T2}$ taking into account the actual volume V of AHS in each sample. Fig. 6(b)-(c) show dependences of entropy ΔS_2 and volume strain $(\Delta V/V)_{T2}$ on the nanoparticle size. It can be seen that at $d_{\text{cryst}} \leq 100$ nm, both values greatly decrease, just as it was found above for the temperatures T_1 and T_2. A rather large difference in the change in the volume strain at T_2 in AHS (~ 1.5 %) and in composites even with rather large-sized particles (~ 1.0 % in AHS+PG160) suggests that the glass matrix prevents the expansion of the ferroelectric component. This is also confirmed by the large difference in the values of α of glass matrices (Fig. 3), nanocomposites (Fig. 5) and bulk AHS [20] in temperature regions far from the phase transitions points.

The temperature dependence of the permittivity of some nanocomposites in comparison with $\varepsilon(T)$ of bulk AHS [20] is shown in Fig. 7. The $\varepsilon(T)$ curves for all samples show specific features characteristic of phase transitions of the first and second order: jump at T_2 and more or less pronounced peak at T_1. At a frequency of $f < 1$ kHz, a strong increase in ε was observed at T > 200 K, which decreased with increasing f to 1 MHz. The increase in the low-frequency permittivity in the nanocomposites with AHS and its strong frequency dependence were also observed in [9,10] and assumed to be associated with the high proton mobility and the appearance of space charge polarization [10].

The temperatures of both phase transitions in all investigated nanocomposites are independent of frequency variation and agree well with those found in calorimetric measurements.

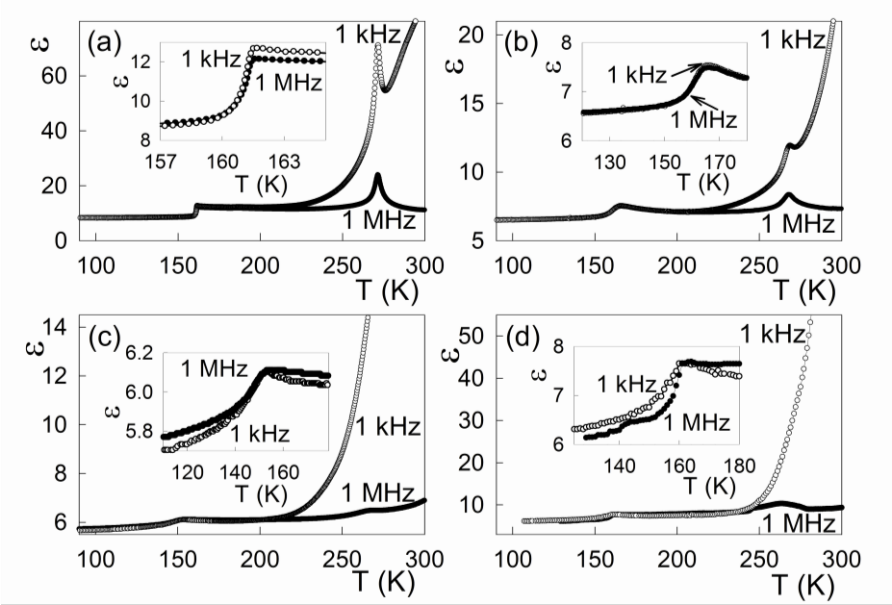

Figure 7 Temperature dependences of permittivity at different f for (**a**) bulk AHS, (**b**) AHS+PG320, (**c**) AHS+PG46, (d) AHS+PG23. Insets show the permittivity behavior near T_2

The values of both the step-wise change in ε at T_2 and the ε peak at T_1 were changed in irregular manner with decreasing pore size, which can be due to both the different filling factor of nanocomposites and the particle size (Table 1). In spite of the smeared ε anomalies in AHS+PG, the peak-like and step-wise behavior of permittivity at T_1 and T_2, respectively, at different frequencies as well as the data on the heat capacity, entropy and thermal expansion prove that the order of both transformations is kept in all the nanocomposites studied.

Similar to studies on bulk ceramic AHS [20], we were not successful in examining the *P*–*E* loops in the three phases of the composite AHS+PG46 (Fig. 8).

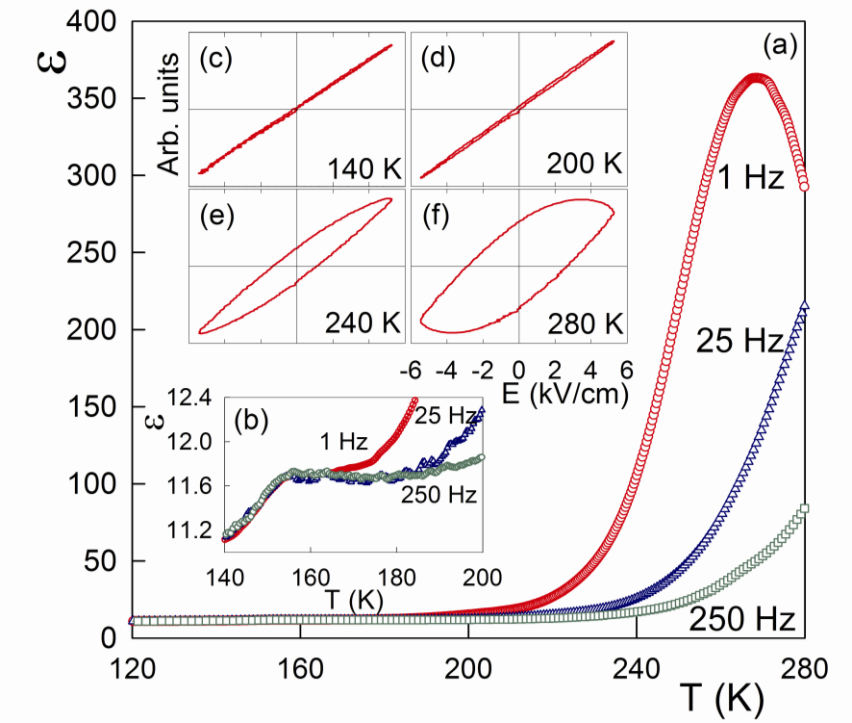

Figure 8 (**a**)-(**b**) Dependence of permittivity on temperature for AHS+PG46 at different frequencies; (**c**)-(**f**) Dielectric hysteresis loops at the corresponding temperatures

A rather strong relaxation in the appearance of *P* in the ferroelectric *Pc* phase was found which was confirmed by an almost linear dependence of polarization versus electric field existed far above T_2 (Fig. 8(c)-(d)). The nonclassical shape of the loops interfered with the correct determination of the polarization. The most probable cause of this is associated with high electrical conductivity, which was observed even in AHS single crystals [26].

The hydrostatic pressure effect on the successive phase transitions $P2_1/c \leftrightarrow Pc \leftrightarrow P\text{-}1$ in AHS and AHS+PG320 was studied by the DTA and permittivity measurements.

The permittivity of both samples measured at a frequency f = 1 kHz and different pressures is presented in Fig. 9. Comparison of these data with those shown in Fig. 7 indicates a strong smearing of the ε anomaly associated with the second order transformation $P2_1/c \leftrightarrow Pc$ in AHS+PG320.

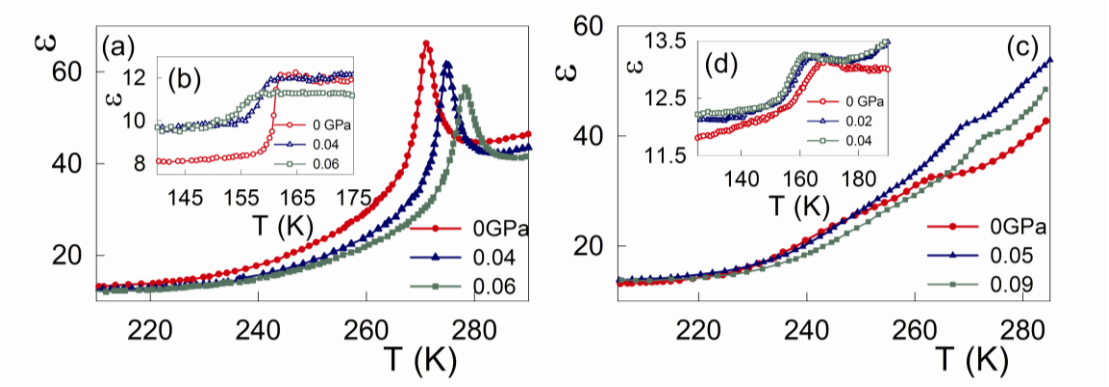

Figure 9 Temperature dependences of permittivity for (**a, b**) AHS Melt and (**c, d**) AHS+PG320 measured upon heating at different pressures. Insets show behavior of ε near T_2

Nevertheless, one can see that the increase in pressure results in a positive shift of T_1 in composite like bulk AHS. At the same time, T_2 decreases under external pressure in both samples. One can assume that the difference in the susceptibility of both temperatures to hydrostatic pressure is associated with different order and origin of the phase transitions in AHS, and as a result with different mechanism of structural distortions [18,27-29].

The results of the DTA measurements under pressure on bulk AHS and AHS+PG320 in the region of the P-1 ↔ Pc phase transition are shown in Fig. 10(a)-(b).

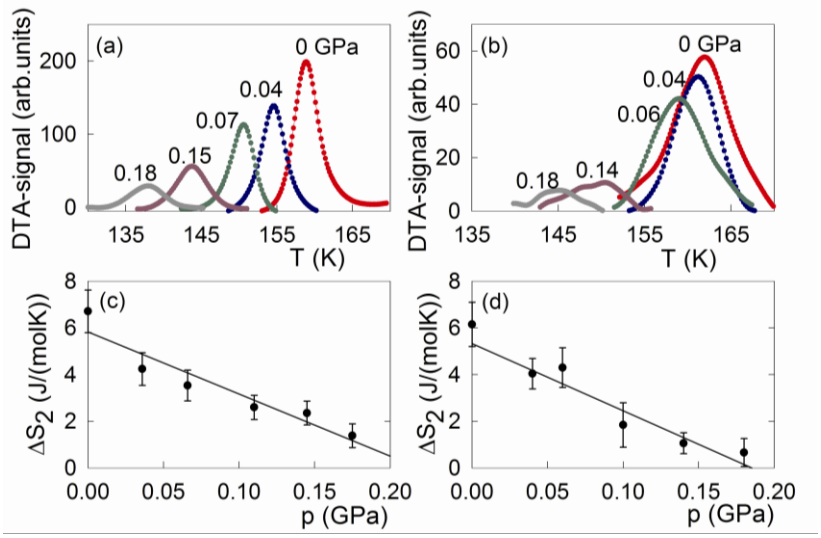

Figure 10 (**a, b**) Anomalous component of the DTA signal near T_2 at different pressures in AHS and AHS+PG320, respectively. (**c, d**) Entropy change ΔS_2 at the first-order transition in bulk AHS and AHS+PG320, respectively. The lines in (**c**) and (**d**) represent linear fits

The increase in pressure is accompanied by a significant reduction of the area under the DTA-signal peaks which is proportional to the entropy change ΔS_2 associated with the phase transition at T_2. The dependences $\Delta S_2(p)$ can be considered as linear with very close values of the coefficient $d\Delta S_2/dp$ = 30 J×(mol×K×GPa)$^{-1}$ and 35 J×(mol×K×GPa)$^{-1}$ for AHS and AHS+PG320, respectively. Such a behavior of $\Delta S_2(p)$ correlates with decrease of ΔS_2 at the particle size reduction found in calorimetric experiments on the nanocomposites (Fig. 6b). Linear and strong nonlinear dependences $\Delta S_2(p)$ and $\Delta S_2(d_{cryst})$ show that decrease in the nanoparticle size is accompanied by strong nonlinear increase in the internal stress between the matrix and the AHS component.

The data on the susceptibility of T_1 and T_2 to hydrostatic pressure in bulk AHS and some nanocomposites are summarized in Table 2. Due to opposite sign of baric coefficients ($dT_1/dp > 0$ and $dT_2/dp < 0$) the temperature interval of ferroelectric *Pc* phase existence is expanding under external pressure.

Table 2 Comparison of susceptibility of phase transitions temperatures to hydrostatic pressure. $(dT_i/dp)_{exp}$ and $(dT_i/dp)_{calc}$ are experimental and calculated baric coefficients, respectively

Sample	d_{cryst} (nm)	T_1 (K)	$(dT_1/dp)_{exp}$ (K/GPa)	T_2 (K)	$(dT_2/dp)_{exp}$ (K/GPa)	$(dT_2/dp)_{calc}$ (K/GPa)
AHS	Bulk	270.5 ± 0.2	90 ± 15	159.0 ± 0.2	- 123 ± 10	- 143 ± 20
AHS+PG160	500	268.0 ± 0.2		161.0 ± 0.2		- 98 ± 15
AHS+PG320	115	263.0 ± 0.5	115 ± 20	161.0 ± 0.2	- 88 ± 12	- 72 ± 15
AHS+PG23	70	260.0 ± 1.0		156.0 ± 0.5		- 45 ± 15
AHS+PG46	47	258.0 ± 0.5	86 ± 20	151.0 ± 0.5	- 78 ± 12	- 56 ± 15
AHS+PG5	9	251.0 ± 2.0		150.0 ± 1.0		~ (- 130)

Taking into account the uncertainty in the experimental determination of $(dT_1/dp)_{exp}$, one can assume that this value changes insignificantly with a change of the nanoparticle size. More pronounced effect was observed in reduction of the $(dT_2/dp)_{exp}$ magnitude depending on d_{cryst}. Using the data on the entropy ΔS_2 and strain $(\Delta V/V)_{T2}$ at the first order phase transition *P*-1 ↔ *Pc* (Fig. 6b), we have also evaluated the baric coefficient dT_2/dp for all the samples under study in the framework of the Clausius-Clapeyron equation (Table 2). It is seen that the values $|dT_2/dp|_{calc}$ are decreased except AHS+PG5, where very large baric coefficient can be due to large error in determination of the strain change $(\Delta V/V)_{T2}$.

The evaluation of the dT_1/dp baric coefficient was not carried out because of strong smeared anomalies of heat capacity and coefficient of the thermal expansion at T_1 in the nanocomposites.

There is a good agreement of the T_2 dependence on the pores size in AHS+PG observed in the present paper and in previous studies [9,10]. However, we found a rather strong decrease in T_1 with decreasing d_{cryst} contrary to [9,10] where this value was observed almost constant.

Let us compare the data on impact of the d_{cryst} size and external pressure on the phase transitions temperatures in AHS+PG. One can suggest two mechanisms leading to the common and specific features in the behavior of T_1 and T_2. One of them is associated with a large difference in the nonanomalous thermal expansion of AHS and PG ($\alpha_{AHS} > \alpha_{PG}$) leading to the appearance of the tensile stresses in ferroelectric component. This mechanism probably plays the primary role in the samples with $d_{cryst} > 100$ nm. Contrary to hydrostatic pressure effect (Table 2), T_1 and T_2 in these nanocomposites were found decreased and increased, respectively, compared to bulk AHS. The value of internal pressure was evaluated using the data on T_2 in AHS and AHS+PG160 and dT_2/dp for AHS. It was found that the increase in T_2 observed in composite (2 K) at the absence of external pressure can be generated by negative pressure of about – 0.015 GPa.

Another mechanism for changing the temperature of phase transitions in ferroelectric nanoparticles is associated with a change in the balance between the short and long interactions [30-32]. We assume that this mechanism plays a predominant role in composites with a small particle size, $d_{cryst} < 100$ nm. Indeed, both T_1 and T_2 decrease with decreasing d_{cryst}. The data presented in Table 2` support this point.

4. Conclusions

Heat capacity, thermal dilatation, susceptibility to hydrostatic pressure and dielectric properties of the series of the nanocomposites AHS+PG were investigated. In order to be correct analyzing experimental data, thermal properties of porous glasses were also studied for the first time.

X-ray characterization has shown the formation of the dendrite clusters with the size exceeding the pore size in some AHS+PG like it was observed in the nanocomposites with the embedded $NaNO_2$ [4].

A distinct difference between nonanomalous coefficients of the thermal expansion in AHS+PG samples is associated with different filling factor and nanoparticle size, d_{cryst}. Rather small anisotropy of the $\alpha(T)$ dependences measured along three directions of the nanocomposite plate confirms the statistically homogeneous distribution of AHS over the volume of a matrix with equiprobable orientations of crystalline nanoparticles.

All investigated properties show anomalous behavior associated with the succession of the two phase transitions $P\text{-}1 \leftrightarrow Pc \leftrightarrow P2_1/c$ which depends mainly on d_{cryst}. The specific features of the phase transition temperatures T_1 and T_2 on d_{cryst} are related for at least two reasons: tensile stresses in the nanocomposites and a size effect. The difference in the susceptibility of both temperatures to external pressure can be due to the different order and origin of the phase transitions in AHS, and as a result to different mechanism of structural distortions.

A significant reduction in the value of the entropy ΔS_2 and volume strain $(\Delta V/V)_{T2}$ at the $P\text{-}1 \leftrightarrow Pc$ transformation with the d_{cryst} decrease can be explained by decrease in disorder of structural elements in the initial phase $P2_1/c$ of AHS confined in glass matrix.

Effect of internal pressure associated with a decrease in d_{cryst} and external hydrostatic pressure on permittivity are similar and accompanied with decrease in the anomalous ε changes at T_1 and T_2 which however can be reliably detected even in a sample of d_{cryst} = 70 nm (d = 23 nm).

The reason of inability to measure polarization is the high electrical conductivity in the nanocomposites observed even in the single crystal of AHS [26].

Hydrostatic pressure leads to a significant linear reduction in the entropy associated with the phase transition $P\text{-}1 \leftrightarrow Pc$ in AHS and AHS+PG320. The decrease in ΔS_2 under hydrostatic pressure is consistent with the behavior of ΔS_2 with the particle size reduction.

We did not observe any effect of pores size and hydrostatic pressure on the order of both phase transitions in nanocomposites AHS+PG.

Acknowledgements

The reported study was funded by Russian Foundation for Basic Research (RFBR) according to the research project No. 16-32-00092 mol_a.

Compliance with ethical standards

Conflicts of interest The authors declare that they have no conflicts of interest.

References

[1] Gutina A, Antropova T, Rysiakiewicz-Pasek E, Virnik K, Feldman Yu (2003) Dielectric relaxation in porous glasses. Micropor Mesopor Mater 58:237-254

[2] Kumzerov Y, Vakhrushev S (2007) Nanostructures within porous materials. In: Nalwa HS (ed) Encyclopedia of Nanoscience and Nanotechnology. American Scientific Publishers; New-York, pp.1-39

[3] Kinka M, Banys J, Naberezhnov A (2007) Dielectric properties of sodium nitrite confined in porous glass. Ferroelectrics 348:67-74

[4] Fokin A, Kumzerov Yu, Koroleva E, Naberezhnov A, Smirnov O, Tovar M, Vakhrushev S, Glazman M (2009) Ferroelectric phase transitions in sodium nitrite nanocomposites. J Electroceram 22:270-275

[5] Rogazinskaya OV, Milovidova SD, Sidorkin AS, Popravko NG, Bosykh MA, Enshina VS (2010) Dielectric properties of ferroelectric composites with TGS inclusions. Ferroelectrics 397:191-197

[6] Tarnavich V, Korotkov L, Karaeva O, Naberezhnov A, Rysiakiewicz-Pasek E (2010) Effect of restricted geometry on structural phase transitions in KH_2PO_4 and $NH_4H_2PO_4$ crystals. Optica applicata 40:305-309

[7] Rogazinsksya OV, Sidorkin AS, Milovidova SD, Naberezhnov AA, Matveev NN, Popravko NG, Fokin AV (2010) Ferroelectricity in nanocomposites based on porous glass with inclusions of $NaNO_2$. Bull Russ Acad Sci Phys 75:1327-1330

[8] Cizman A, Antropova T, Anfimova I, Drozdova I, Rysiakiewicz-Pasek E, Radojewska EB, Poprawski R (2013) Size driven ferroelectric-paraelectric phase transition in TGS nanocomposites. J Nanopart Res 15:1807(6pp)

[9] Cizman A, Marciniszyn T, Enke D, Barascu A, Poprawski R (2013) Phase transition in NH_4HSO_4–porous glasses nanocomposites. J Nanopart Res 15:1756(7pp)

[10] Baryshnikov SV, Milinskiy AYu, Charnaya EV, Bugaev AS, Samoylovich MI (2016) Dielectric studies of ferroelectric NH_4HSO_4 nanoparticles embedded into porous matrices. Ferroelectrics 493:85-92

[11] Kutnjak Z, Vodopivec B, Blinc R, Fokin AV, Kumzerov YA, Vakhrushev SB (2005) Calorimetric and dielectric studies of ferroelectric sodium nitrite confined in a nanoscale porous glass matrix. J Chem Phys 123:084708

[12] Rysiakiewicz-Pasek E, Poprawski R, Polanska J, Urbanowicz A, Sieradzki A (2006) Properties of porous glasses with embedded ferroelectric materials. J Non-Crystalline Solids 352:4309-4314

[13] Kumzerov YuA, Kartenko NF, Parfen'eva LS, Smirnov IA, Fokin AV, Wlosewicz D, Misiorek H, Jezowski A (2011) Capacity and thermal conductivity of a nanocomposite chrysolite asbestos–KDP (KH_2PO_4). Phys Solid State 53**:**1099-1103

[14] Cizman A, Marciniszyn T, Poprawski R (2012) Pressure effect on the ferroelectric phase transition in nanosized NH_4HSO_4. J Appl Phys 112:034104

[15] San-Miguel A (2006) Nanomaterials under high-pressure. Chem Soc Rev 35:876-889

[16] R. Pepinsky, K. Vedam, Y.S. Okaya, S. Hosino (1958) Ammonium hydrogen sulfate: a new ferroelectric with low coercive field. Phys Rev 111 1508-1510

[17] Flerov IN, Zinenko VI, Zherebtsova LI, Iskornev IM, Blat DCh (1975) Study of phase transitions in ammonium hydrosulfate. Izvestiya AN USSR (seriya fizicheskaya) 39:752-757

[18] Swain D, Bhadram VS, Chowdhury P, Narayana C (2012) Raman and X-ray Investigations of Ferroelectric Phase Transition in NH_4HSO_4. J Phys Chem A 116**:**223-230

[19] Mikhaleva EA, Flerov IN, Bondarev VS, Gorev MV, Vasiliev AD, Davydova TN (2011) Phase transitions and caloric effects in ferroelectric solid solutions of ammonium and rubidium hydrosulfates. Phys Solid State 53:510-517

[20] Mikhaleva EA, Flerov IN, Kartashev AV, Gorev MV, Bogdanov EV, Bondarev VS (2017) Thermal, dielectric and barocaloric properties of NH_4HSO_4 crystallized from an aqueous solution and the melt. Solid State Sci 67:1-7

[21] Kosova DA, Emelina AL, Bykov MA (2014) Phase transitions of some sulfur-containing ammonium salts. Thermochimica Acta 595:61-66

[22] Bruker. AXS TOPAS V4 (2008) General profile and structure analysis software for powder diffraction data – User's Manual, Bruker AXS, Karlsruhe, Germany

[23] Kartashev AV, Flerov IN, Volkov NV, Sablina KA (2008) Adiabatic calorimetric study of the intense magnetocaloric effect and the heat capacity of $(La_{0.4}Eu_{0.6})_{0.7}Pb_{0.3}MnO_3$. Phys Solid State 50:2115-2120

[24] Shimizu H, Abe N, Yasuda N, Fujimoto S, Sawada S, Shiroishi Y (1979) Differential Thermal Analysis Using a Ge–Ag Thermocouple under Hydrostatic Pressure: Phase Behavior of $\{N(CH_3)_4\}_2MnCl_4$. Jpn J Appl Phys 18:857-858

[25] Iskornev IM, Flerov IN (1978) Thermal expansion of ferroelectric crystals of the ammonium hydrosulfate family. Fizika Tverdogo Tela 20:2649-2653

[26] Flerov IN, Mikhaleva EA (2008) Electrocaloric Effect and Anomalous Conductivity of the Ferroelectric NH_4HSO_4. Phys Solid State 50:478-484

[27] Miller R, Blinc R, Brenman M, Waugh JS (1962) Nuclear spin-lattice relaxation in some ferroelectric ammonium salts. Phys Rev 126:528-532

[28] Nelmes RJ (1971) An X-ray diffraction determination of the crystal structure of ammonium hydrosulfate above the ferroelectric transition. Acta Crystallogr B27**:**272-281

[29] Nelmes RJ (1972) The structure of ammonium hydrogen sulfate in its ferroelectric phase and the ferroelectric transition. Ferroelectrics 4:133-140

[30] Kretschmar R, Binder K (1979) Surface effects on phase transitions in ferroelectrics and dipolar magnets. Phys Rev B20:1065-1076

[31] Tilley DR, Zeks B (1984) Landau theory of phase transitions in thick films. Solid State Commun 49:823-828

[32] Ishikawa K, Yoshikawa K, Okada N (1988) Size effect on the ferroelectric phase transition in $PbTiO_3$ ultrafine particles. Phys Rev B37:5852-5855